



OPEN

Sulfamic acid pyromellitic diamide-functionalized MCM-41 as a multifunctional hybrid catalyst for melting-assisted solvent-free synthesis of bioactive 3,4-dihydropyrimidin-2-(1*H*)-ones

Ehsan Valiey, Mohammad G. Dekamin[✉] & Zahra Alirezvani

This study introduces a practical approach to fabricate a novel hybrid acidic catalyst, namely sulfamic acid pyromellitic diamide-functionalized MCM-41 (MCM-41-APS-PMDA-NHSO₃H). Various techniques such as FTIR, TGA, XRD, BET, FESEM, and EDX were used to confirm its structural characteristics. The efficiency of the new MCM-41-APS-PMDA-NHSO₃H organosilica nanomaterials, as a heterogenous nanocatalyst, was examined in the synthesis of biologically active 3,4-dihydropyrimidin-2-(1*H*)-one derivatives under solvent-free conditions. It was found that the nanoporous MCM-41-APS-PMDA-NHSO₃H, demonstrating acidic nature and high surface area, can activate all the Biginelli reaction components to afford desired 3,4-dihydropyrimidin-2-(1*H*)-ones under solvent-free conditions in short reaction time. Furthermore, easy and quick isolation of the new introduced hybrid organosilica from the reaction mixture as well as its reusability with negligible loss of activity in at least five consecutive runs are another advantages of this green protocol.

In recent decades, the synthesis and use of mesoporous structures have received much attention. The M41S family consists mainly of silica, SiO₂. Silica has certain advantages such as high chemical and thermal stability, large number of silanol (Si–OH) groups and simplicity of operation, which have made it an appropriate and well-known support in the chemical industry. MCM-41 became the most attractive member of the M41S family due to its ordered structure and special properties such as exceptional high surface area (> 1000 m² g⁻¹) and narrow pore-size distribution (1.5–10 nm)^{1–4}. These properties have made MCM-41 as an appropriate nanomaterial support for metal oxides⁵, heteropoly acids⁶, metal–ligand complexes^{7,8}, etc. to immobilize catalytic active centers^{9–13} as well as to develop more efficient drug delivery systems^{14–18}, sensors¹⁹, degradation inhibitors in polymer industry²⁰, adsorbents of organic pollutants^{21–23}. However, the acidic strength of the pure MCM-41 is relatively weak, which hinders its catalysis applications. Therefore, modification of its surface can lead to the formation of solid acids with high uniformity, which are regularly prepared by covalent anchoring of various organic moieties with proper functional groups in a mesoporous material or replacing of Si atoms by other tetra-, tri- and divalent metals such as Al, B, Fe, Mn, Zn, etc.^{16,24–40}. Hence, covalent anchoring of both sulfamic and pyromellitic acids in the pore walls of MCM-41 can significantly enhance the catalytic capabilities of the designed catalyst.

On the other hand, solvent-free organic synthesis (SFOS) has been emerged as an effective tool for the rapid preparation of various organic compounds especially biologically active molecules during recent years⁴¹. In fact, solvent-free conditions obviously form a liquid phase on heating of the reaction mixture with solid substrates. This melting mentions the eutectic mixture with temperature fusion below the melting points of the reactants. These solvent-free protocols have many advantages including the products are sufficiently pure which does not require further purification or recrystallization; the reactions are sometimes rapid as compared to conditions using often toxic solvents; functional group protection–deprotection can be avoided, and sometimes the use of solvent-free conditions is more inexpensive^{42,43}. Furthermore, the use of multicomponent reactions (MCRs)

Pharmaceutical and Heterocyclic Compounds Research Laboratory, Department of Chemistry, Iran University of Science and Technology, 16846-13114 Tehran, Iran. ✉email: mdekamin@iust.ac.ir

allows formation of densely functionalized organic molecules such as dihydropyrimidinones (DHPMs) in a simple synthetic procedure^{43–47}. Hence, the simultaneous use of solid acids, solvent-free conditions and MCRs would be very beneficial to prepare high-value organic compounds as well as address green chemistry principles⁴⁸.

In the past few decades, dihydropyrimidinones (DHPMs) and their derivatives, as an important class of heterocyclic compounds, have stimulated interest in medicinal chemistry due to their diverse biological activities^{48–51}. These pyrimidine-containing heterocycles are present significantly in natural products or synthetic organic compounds such as natural marine polycyclic guanidine alkaloids, the kinesin Eg5 inhibitor Monastrol, BACE-1 inhibitor to prevent Alzheimer's disease, bioprobes and fluorescent sensors^{51–55}. Due to important properties of DHPMs, different methods using Brønsted or Lewis acids catalysts have been developed for the synthesis of DHPMs by the Biginelli reaction in recent years^{55–59}. Among these catalytic systems, the immobilization of the catalytic active centers on a wide range of solid polymer supports, especially silica, can improve the efficiency of the relevant method^{59–63}. In continuation of our ongoing efforts towards developing of more efficient heterogeneous catalysts for different MCRs^{63–70}, we wish herein to introduce preparation and characterization of the new hybrid sulfamic acid pyromellitic diamide-functionalized MCM-41 (MCM-41-APS-PMDA-NHSO₃H) nanomaterials. Also, its catalytic activity was investigated in the three-component synthesis of 3,4-dihydropyrimidin-2-(1*H*)-one derivatives from aromatic aldehydes, ethyl acetoacetate and urea (Scheme 1). To the best of our knowledge, there is not any report for the use of sulfamic acid pyromellitic diamide grafted on the surface of MCM-41, as a heterogeneous nanocatalyst, for the synthesis of Biginelli 3,4-dihydropyrimidin-2-(1*H*)-one derivatives.

Results and discussion

Characterization of the MCM-41-APS-PMDA-NHSO₃H nanomaterials (1). The as prepared MCM-41-APS-PMDA-NHSO₃H nanomaterial was analyzed using different spectroscopic, microscopic and analytical methods as well as porosimetric and porometric techniques including FTIR, EDX, XRD, FESEM, TGA and BET experiments. The FTIR spectra of MCM-41 (a), MCM-41-APS (b) MCM-41-APS-PMDA (c) and MCM-41-APS-PMDA-NHSO₃H are show in Fig. 1. The nano-ordered MCM-41 shows a band in the 3443 cm⁻¹ region that is due to the presence of both Si–OH and OH groups of the adsorbed water molecules on its surface (Fig. 1a)⁷¹. Furthermore, the band corresponded to Si–O–Si bonds for MCM-41 and all subsequent modifications are observed around 1228–1062 cm⁻¹. Also, the signals in the regions of 1600 cm⁻¹ and 2883 cm⁻¹ are attributed to the symmetric vibrations of NH₂ and the asymmetric vibrations of C–H of 3-APTS, respectively (Fig. 1b). On the other hand, the decrease in signal intensity of the OH groups of MCM-41 surface confirms that the MCM-41 substrate has been modified by the covalent bonding of the 3-APTS linker. In addition, the observed broad band at 3604–2923, 1716 and 1569 cm⁻¹ are attributed to the stretching vibrations of the pyromellitic acid and its amide derivative (Fig. 1c). Also, the characteristic band observed at 1365 and 1066 cm⁻¹ are assigned to the asymmetric and symmetric S=O stretching vibration of the SO₃H group (Fig. 1d).

Also, the morphology and textural properties of the MCM-41 and MCM-41-APS-PMDA-NHSO₃H (1) were examined using field emission scanning electron microscopy (FESEM). As shown in Fig. 2, the morphological distinction between the pure MCM-41 (2a–c images) and MCM-41-APS-PMDA-NHSO₃H (1, 2d–f images) demonstrate grafting of the *N*-carbonyl sulfamic acid pyromellitic diamide moiety on the outer surface of MCM-41 support.

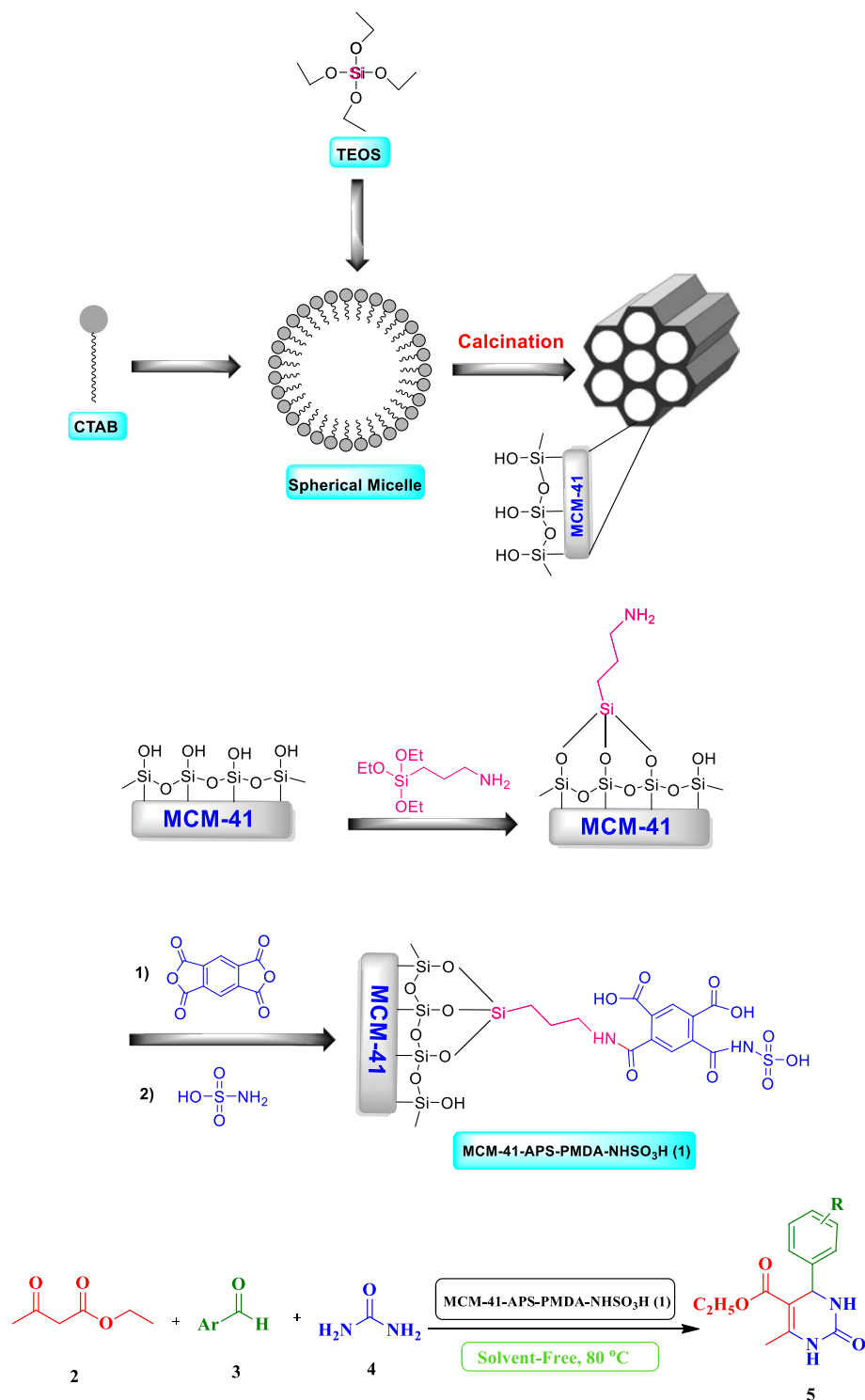
On the other hand, the thermogravimetric analysis (TGA) of the MCM-41-APS-PMDA-NHSO₃H (1) are shown in Fig. 3. The TGA curve of MCM-41-APS-PMDA-NHSO₃H shows three distinct steps of weight loss. In the first step, 10% weight loss between 50 °C and 150 °C can be attributed to the absorbed water or solvent molecules held in the pores of the MCM-41-APS-PMDA-NHSO₃H nanomaterial. The second weight loss between 150 and 350 °C is due to decomposition of the grafted organic *N*-carbonyl sulfamic acid pyromellitic diamide moiety. Also, the third weight loss (17%) between 380 and 600 °C can be related to the conversion of silanol (Si–OH) groups to siloxane (Si–O–Si) bridges. These results also indicate that the *N*-carbonyl sulfamic acid pyromellitic diamide moiety has successfully been grafted onto the surface of MCM-41.

As shown in Fig. 4, the energy-dispersive X-ray (EDX) spectra of the MCM-41-APS-PMDA-NHSO₃H (1) verified the presence of Si (11.61%), C (14.89%), O (57.63%), N (12.90%), and S (2.98%), respectively.

Furthermore, the powder XRD pattern of the MCM-41-APS-PMDA-NHSO₃H (1, Fig. 5a) shows low angle reflections of (d100), (d110) and (d200) at 2θ = 2.77°, 4.67° and 5.13°, respectively. These plates confirm the formation of a hexagonal mesoporous structure with regular particle size and pores, which indicates its structure is similar to the mesoporous MCM-41 precursor. On the other hand, the observed peaks in the wide angle XRD pattern are in well agreement with both Joint Committee on Powder Diffraction Standards (JCPDS) card no 00-003-0268 (sulfamic acid) and 00-024-1864 (pyromellitic dianhydride). These data also demonstrate successful grafting of the the organic moieties onto the surface of nanocatalyst 1. Indeed, the diffraction signals observed at 2θ = 14.0°, 19.0°, 23.0°, 25.0°, 26.0°, 29.3° illustrates the formation of MCM-41-APS-PMDA-NHSO₃H (Fig. 5b).

Figure 6 demonstrates the N₂ adsorption/desorption isotherms of the MCM-41, MCM-41-APS-PMDA-NHSO₃H. Isotherm type V was recognizable for MCM-41-APS-PMDA-NHSO₃H with hysteresis loop. The table shows the parameters such as pore volume as well as average pore diameter in MCM-41 and the nanocatalyst 1. In fact, grafting of APS-PMDA-NHSO₃H groups through the (3-aminopropyl) triethoxysilane and pyromellitic acid linkers reduces both surface area and pore volume whereas increases pore diameter of the nanocatalyst 1.

Investigation of the catalytic activity of the MCM-41-APS-PMDA-NHSO₃H nanocatalyst (1) for the synthesis of 3,4-dihydropyrimidinones 5a–k. To evaluate the catalytic activity of the MCM-41-APS-PMDA-NHSO₃H nanomaterials (1) in the synthesis of 3,4-dihydropyrimidin-2(1*H*)-ones, the reaction of ethyl acetoacetate (2, 1 mmol), 4-chlorobenzaldehyde (3a, 1 mmol) and urea (4, 1.2 mmol) was investigated as



Scheme 1. Schematic preparation of MCM-41-APS-PMDA-NHSO₃H (1) for the three-component condensation of ethyl acetoacetate (2), aldehydes (3), urea (4) to afford 3,4-dihydropyrimidin-2-(1H)-one derivatives (5).

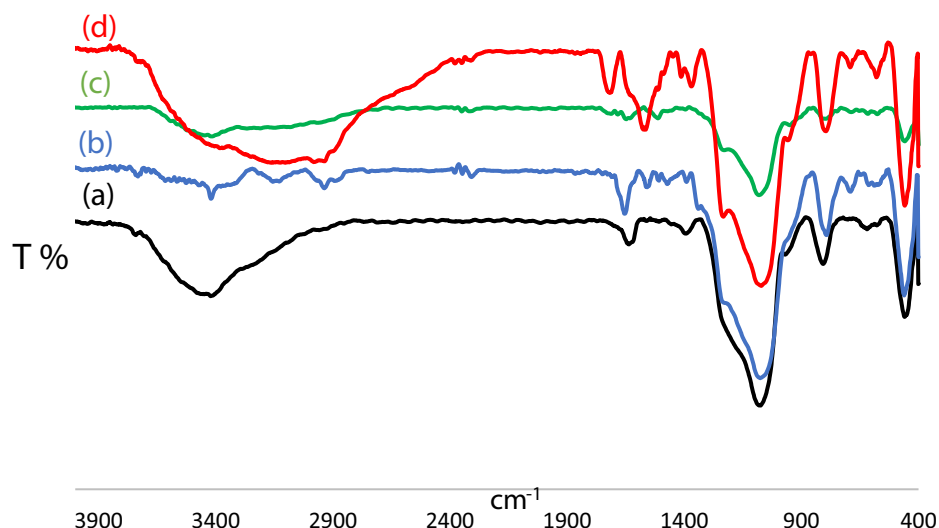


Figure 1. FTIR spectra of the MCM-41 (a), MCM-41-APS (b), MCM-41-APS-PMDA (c) and MCM-41-APS-PMDA-NHSO₃H (d) (1).

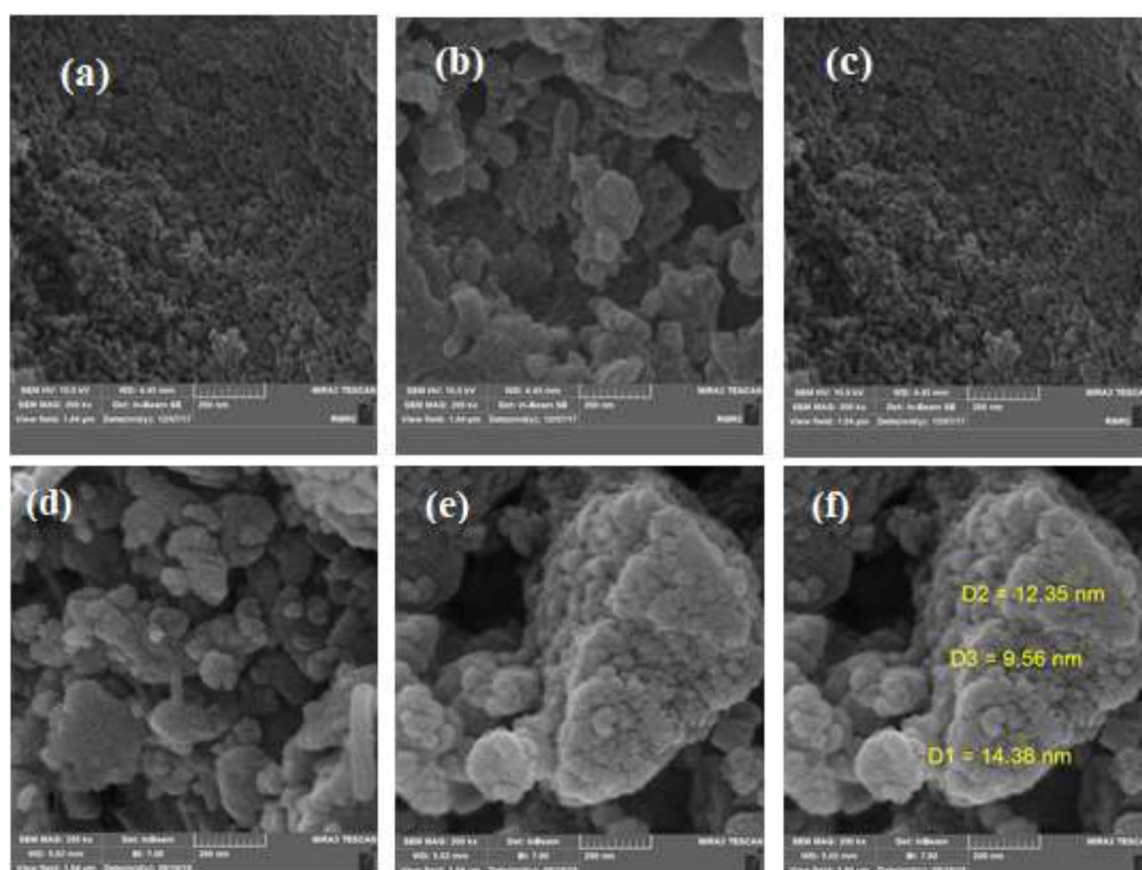


Figure 2. FESEM images of the MCM-41 (a–c) and the MCM-41-APS-PMDA-NHSO₃H (1, d–f) materials.

the model reaction under different conditions. A systematic study was performed to optimize different parameters affecting of the model reaction such as solvent, catalyst loading and temperature. The results are summarized in Table 1. The results of using different polar and non-polar solvents as well as solvent-free conditions showed that the model reaction proceeded very well with lower catalyst **1** loading under solvent-free conditions at 80 °C in shorter reaction time (Table 1, entries 1–11). These findings encouraged us to perform the model reaction under solvent-free conditions in further optimization reactions (entries 12–14). Indeed, by further

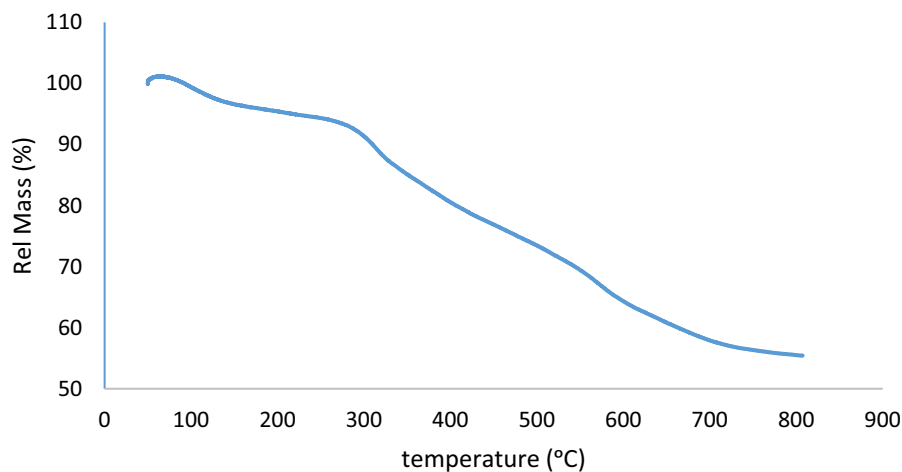


Figure 3. TGA analysis of the MCM-41-APS-PMDA-NHSO₃H materials (**1**).

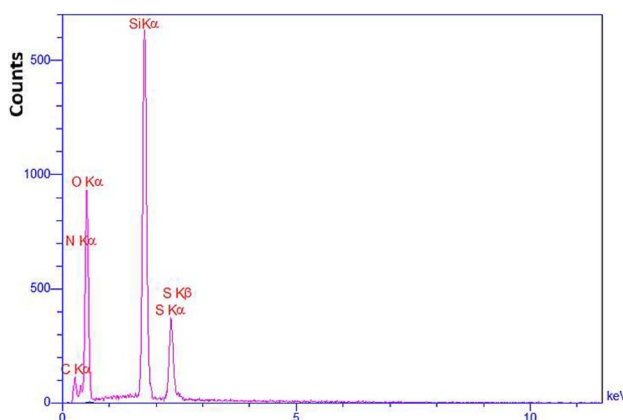


Figure 4. EDX spectra of the MCM-41-APS-PMDA-NHSO₃H materials (**1**).

reducing of the catalyst loading, lower yields of the desired product ethyl 4-(4-chlorophenyl)-6-methyl-2-oxo-1,2,3,4-tetrahydropyrimidin-5-carboxylate (**5a**) were obtained under similar conditions even over longer times. On the other hand, it is noteworthy that a very low yield of the desired product **5a** was obtained in the absence of the MCM-41-APS-PMDA-NHSO₃H nanomaterials (**1**). Therefore, these results strongly confirmed the role of MCM-41-APS-PMDA-NHSO₃H (**1**) to promote the synthesis of 3,4-dihydropyrimidin-2(1*H*)-ones under solvent-free conditions. Hence, 15 mg of catalyst **1** under solvent-free conditions at 80 °C were selected as the optimal conditions for the next experiments.

The optimized conditions were developed to different carbocyclic or heterocyclic aromatic aldehydes affording other 3,4-dihydropyrimidin-2(1*H*)-one derivatives. The results are summarized in Table 2. Noticeably, the desired products **5a–k** were obtained in high to excellent yields. In fact, aldehydes **3** bearing electron-withdrawing groups on their aromatic ring generally react faster compared to those having electron-donating groups. These results clearly confirm the appropriate catalytic activity of the MCM-41-APS-PMDA-NHSO₃H hybrid nanomaterials (**1**) to promote the Biginelli condensation of a wide range of aldehydes with ethyl acetoacetate and urea.

According to the above results and observations, the following mechanism can be proposed for the synthesis of 3,4-dihydropyrimidin-2(1*H*)-ones derivatives catalyzed by the MCM-41-APS-PMDA-NHSO₃H nanocatalyst (**1**, Scheme 2). Firstly, MCM-41-APS-PMDA-NHSO₃H (**1**) activates the carbonyl group of aromatic aldehyde **3** for the addition of urea **4** on it to form intermediate (**II**). Followed by dehydration of this intermediate, the corresponding iminium intermediate (**IV**) is formed. Then, intermediate (**V**) is produced after addition of the enol form of ethyl acetoacetate (**2'**) on the intermediate (**IV**). Subsequent cyclization of the intermediate (**V**) and final dehydration of intermediate (**VI**) afford corresponding 3,4-dihydropyrimidin-2(1*H*)-ones **5**. Furthermore, eliminated water molecules during the catalytic cycle can be adsorbed on the surface of catalyst **1** and facilitate the reaction.

As a part of our study, the heterogeneous solid acid catalyst **1** was separated from the model reaction mixture after its completion, washed several times with EtOH, and then dried in an oven at 60 °C for 1.5 h. The recycled catalyst **1** was reused in four consecutive model reaction under optimized conditions. The results are shown in

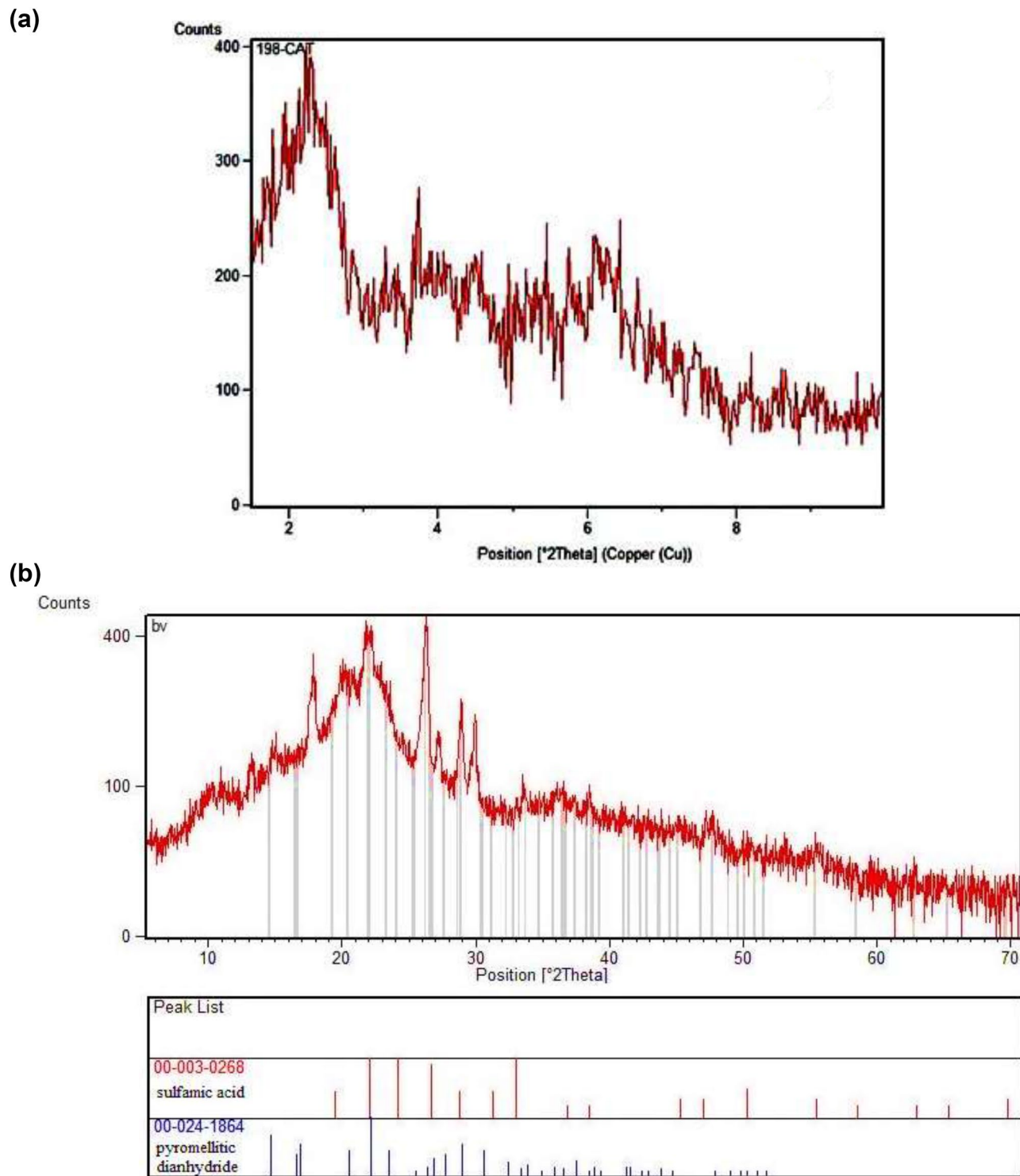


Figure 5. Low angle (a) and wide angle (b) XRD patterns of the hybrid MCM-41-APS-PMDA-NHSO₃H nanocatalyst (**1**).

Fig. 7. Interestingly, only a very little decrease in the catalytic activity of the MCM-41 (MCM-41-APS-PMDA-NHSO₃H (**1**), approx. 10%) was observed.

To illustrate the merits of catalytic activity of the new MCM-41-APS-PMDA-NHSO₃H organosilica nano-materials, as a heterogeneous solid acid, its efficiency has been compared with some of the previously reported catalysts for the preparation of **5a** (Table 3). The results illustrate that this study is actually superior to other cases in terms of desired product yield, amount of catalyst loading, reaction time, working under solvent-free conditions, avoiding of the use of corrosive or expensive reagents and transition metals, and the reusability of the catalyst for at least five consecutive runs.

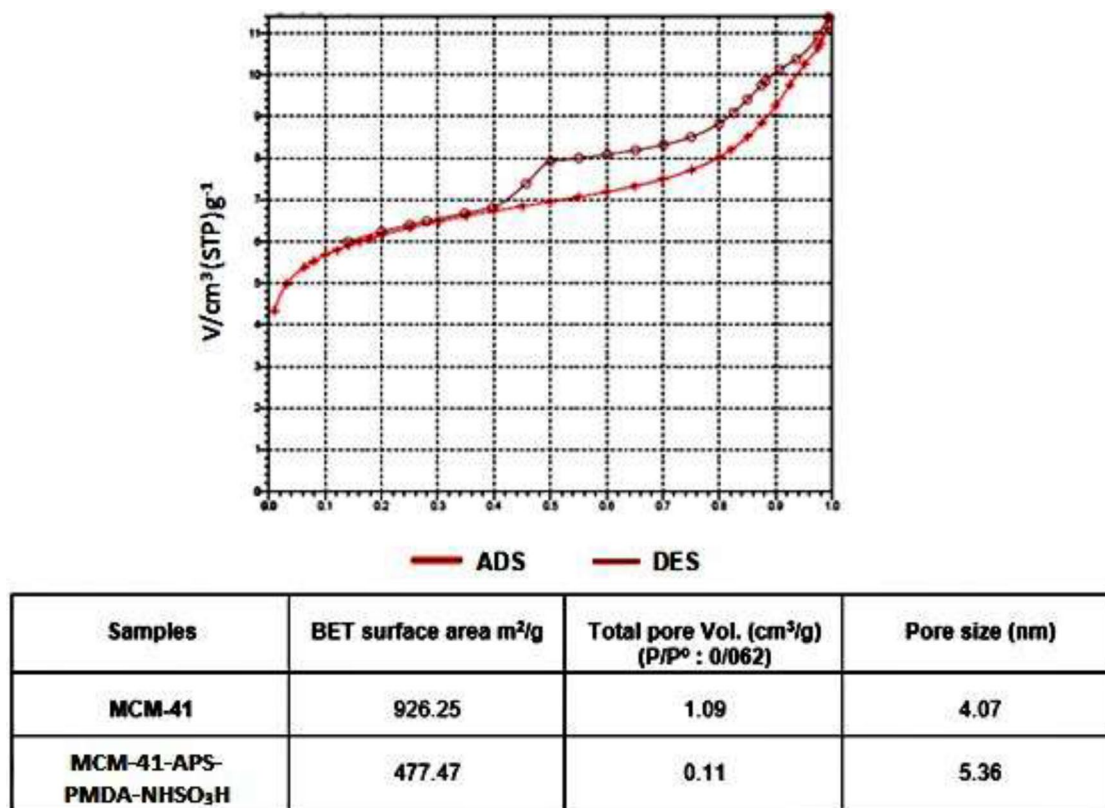


Figure 6. Adsorption/desorption isotherm of the MCM-41-APS-PMDA-NHSO₃H nanocatalyst (1).

Experimental section

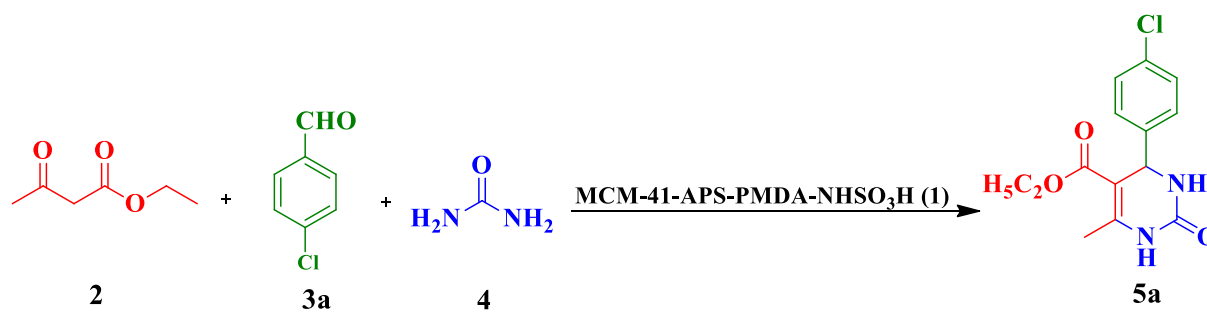
General information. All chemicals were purchased from Merck or Aldrich chemical companies. Melting points were measured using an Electrothermal 9100 device and are unmodified. Characterization of the new hybrid nanocatalyst **1** was performed by FESEM TESCAN-MIRA3, EDX Numerix DXP-X10P, Shimadzu FTIR-8400S and TGA Bahr Company STA 504. The XRD pattern of the catalyst was obtained using a TW 1800 diffractometer with Cu K α radiation ($\lambda = 1.54050 \text{ \AA}$). The analytical thin layer chromatography (TLC) experiments were performed using Merck 0.2 mm silica gel 60F-254Al-plates. All compounds are known and well characterized by FTIR and ¹H NMR (500 MHz, Bruker DRX-500 Avance, in DMSO-d₆ at ambient temperature) spectroscopy.

General procedure for preparation of the MCM-41. Nano-ordered mesoporous silica MCM-41 was prepared by the hydrothermal synthesis and according to known reported method⁸⁶. 2.70 g of diethyl amine was dissolved in 42 mL deionized water at room temperature. The mixture was stirred for 10 min, then 1.47 g of cetyltrimethylammonium bromide (CTAB) was added and the obtained mixture was stirred for 30 min until a clear solution was produced. Next, 2.10 g tetraethyl orthosilicate (TEOS) was gently added and by dropwise addition of HCl solution (1 M), the pH of the mixture was fixed at 8.5 to afford the final precipitate. The resulting mixture was stirred for 2 h and then the resulting white precipitate was filtered and washed with 100 mL of distilled water. Afterward, the obtained white solid was dried at 45 °C for 12 h and finally the sample was calcined at 550 °C with the rate of 2 °C/min for 5 h.

General procedure for preparation of the MCM-41-APS-PMDA-NHSO₃H (1). In a 200 mL round bottom flask, (3-aminopropyl) triethoxysilane (3-APTS, 0.15 mmol, $d = 0.946 \text{ g/mL}$) was added to a mixture of MCM-41 (0.15 g) in dry toluene (15 mL) under stirring and reflux conditions. After 8 h, the obtained white MCM-41-APS solid was filtered, and washed with toluene and CHCl₃ several times to remove any excess of the 3-APTS linker. The MCM-41-APS-NH₂ solid was heated in an oven at 80 °C for 8 h. Next, dried MCM-41-APS-NH₂ solid (0.15 g) and pyromellitic dianhydride (0.15 g) were dispersed in dry THF (30 mL) and the obtained mixture was stirred at r.t for 1 h. Following this, triethylamine (TEA, 0.10 g) was added to the obtained mixture. Then the mixture was stirred at r.t for 24 h under N₂ atmosphere. Afterward, the obtained solid was filtered off and washed with toluene and EtOH (2 mL), respectively, for several times. The as-prepared solid having an anhydride functional group was first dispersed in dry toluene (20 mL) and then triethylamine (0.10 g) and sulfamic acid (0.10 g) were added. The obtained mixture was stirred under N₂ atmosphere and reflux conditions

Entry	Catalyst loading (mg)	Solvent	Temperature (°C)	Time (min)	Yield ^b (%) 5a
1	20	MeOH	r.t	180	26
2	20	EtOH	Reflux	90	69
3	20	CH ₂ Cl ₂	Reflux	90	45
4	20	CH ₃ CN	60	120	78
5	20	DMF	Reflux	100	62
6	20	Toluene	Reflux	150	48
7	20	Et ₂ O	r.t	240	35
8	20	CHCl ₃	60	120	75
9	20	EtOH/H ₂ O (1:2)	Reflux	55	77
10	20	EtOH/H ₂ O (1:1)	Reflux	70	73
11	15	Solvent-free	80	35	95
12	10	Solvent-free	80	65	69
13	5	Solvent-free	80	90	60
14	2	Solvent-free	80	120	57
15	0	Solvent-free	80	180	15

Table 1. Optimization of conditions in the model reaction of ethyl acetoacetate (**2**), 4-chlorobenzaldehyde (**3a**), urea (**4**) under different conditions in the presence of MCM-41-APS-PMDA-NHSO₃H (**1**).^a



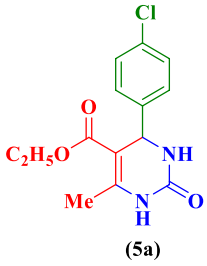
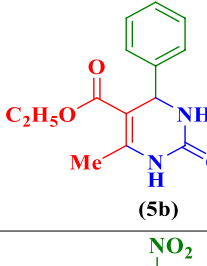
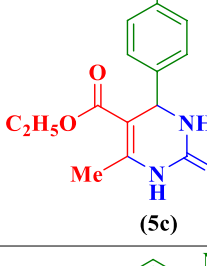
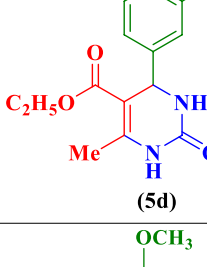
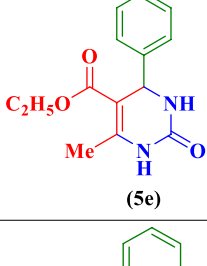
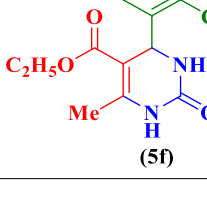
^aReaction conditions: ethyl acetoacetate (**2**, 1 mmol), 4-chlorobenzaldehyde (**3a**, 1 mmol), urea (**4**, 1.2 mmol), MCM-41-APS-PMDA-NHSO₃H (**1**) and solvent (2 ml, if not otherwise stated).

for 36 h. Finally, the white solid was filtered, washed with EtOH (2 mL) for several times and dried in oven at 60 °C for 8 h. The preparation schematic route of the MCM-41-APS-PMDA-NHSO₃H nanomaterials (**1**) has been shown in Scheme 1.

General procedure for the synthesis of 3,4-dihydropyrimidinone-2-(1H)-ones 5a–k catalyzed by the MCM-41-APS-PMDA-NHSO₃H (1**).** In a 5 mL round-bottom flask, a mixture of ethyl acetoacetate (**2**, 1 mmol), aldehydes (**3**, 1 mmol), urea (**4**, 1.2 mmol) and MCM-41-APS-PMDA-NHSO₃H (**1**, 15 mg) was heated at 80 °C under solvent-free conditions for times indicated in Table 2. The progress of the reactions was monitored by TLC (Eluent: EtOAc: n-hexane, 1:3). After completion of the reaction, 96% EtOH (3 mL) was added to the mixture. The heterogeneous catalyst was then separated by filtration and the filtrate was allowed to cool over time to give pure crystals of the desired 3,4-dihydropyrimidinones **5a–k**. The separated catalyst was suspended in EtOH (2 mL) and stirred at r.t for 30 min. Then, it was filtered off and dried in an oven at 60 °C for 1.5 h to be used for next runs.

Conclusions

In summary, we have developed an efficient and practical synthetic methodology for the preparation of 3,4-dihydropyrimidin-2(1H)-ones using sulfamic acid pyromellitic diamide-functionalized MCM-41 (MCM-41-APS-PMDA-NHSO₃H), as a heterogeneous multifunctional hybrid catalyst, under solvent-free conditions. Low catalyst loading, high to quantitative yield of the desired products and compatibility with various functional groups as well as easy and quick isolation of the products from the reaction mixture and reusability of the novel solid acidic hybrid organosilica with negligible loss of its activity are the main advantages of this procedure. Further works to expand and apply MCM-41-APS-PMDA-NHSO₃H nanomaterials in different organic transformations is ongoing in our laboratory and would be presented in due courses.

Entry	Aldehyde 3	Product 5	Time (min)	Yield (%) ^b	mp °C (Obs.)	mp °C (Lit.)
1	4-ClC ₆ H ₄ -	 <p>(5a)</p>	35	95	210–211	210–211 ⁷²
2	C ₆ H ₅ -	 <p>(5b)</p>	55	87	235–236	234–236 ⁷³
3	4-NO ₂ C ₆ H ₄ -	 <p>(5c)</p>	50	80	204	224–227 ⁷⁴
4	3-NO ₂ C ₆ H ₄ -	 <p>(5d)</p>	60	82	293–295	204 ⁷⁵
5	4-CH ₃ OC ₆ H ₄ -	 <p>(5e)</p>	55	89	201–203	202–204 ⁷⁶
6	2-ClC ₆ H ₄ -	 <p>(5f)</p>	60	90	211–213	211–213 ⁷⁵
Continued						

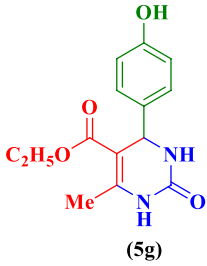
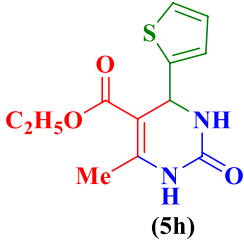
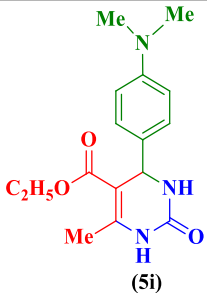
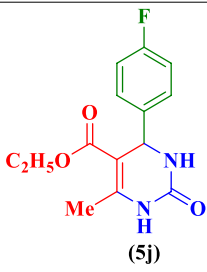
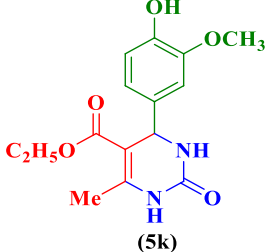
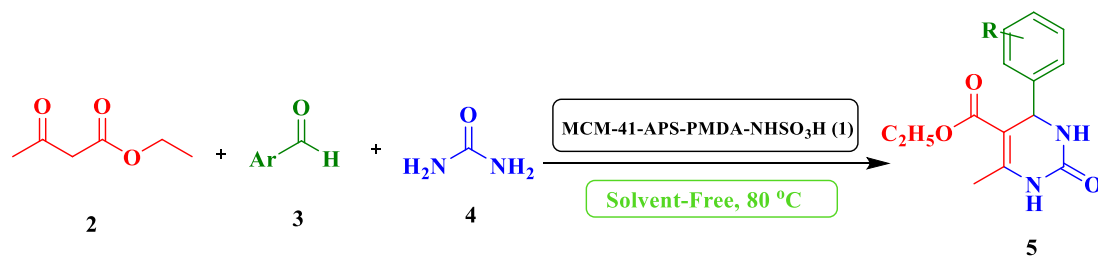
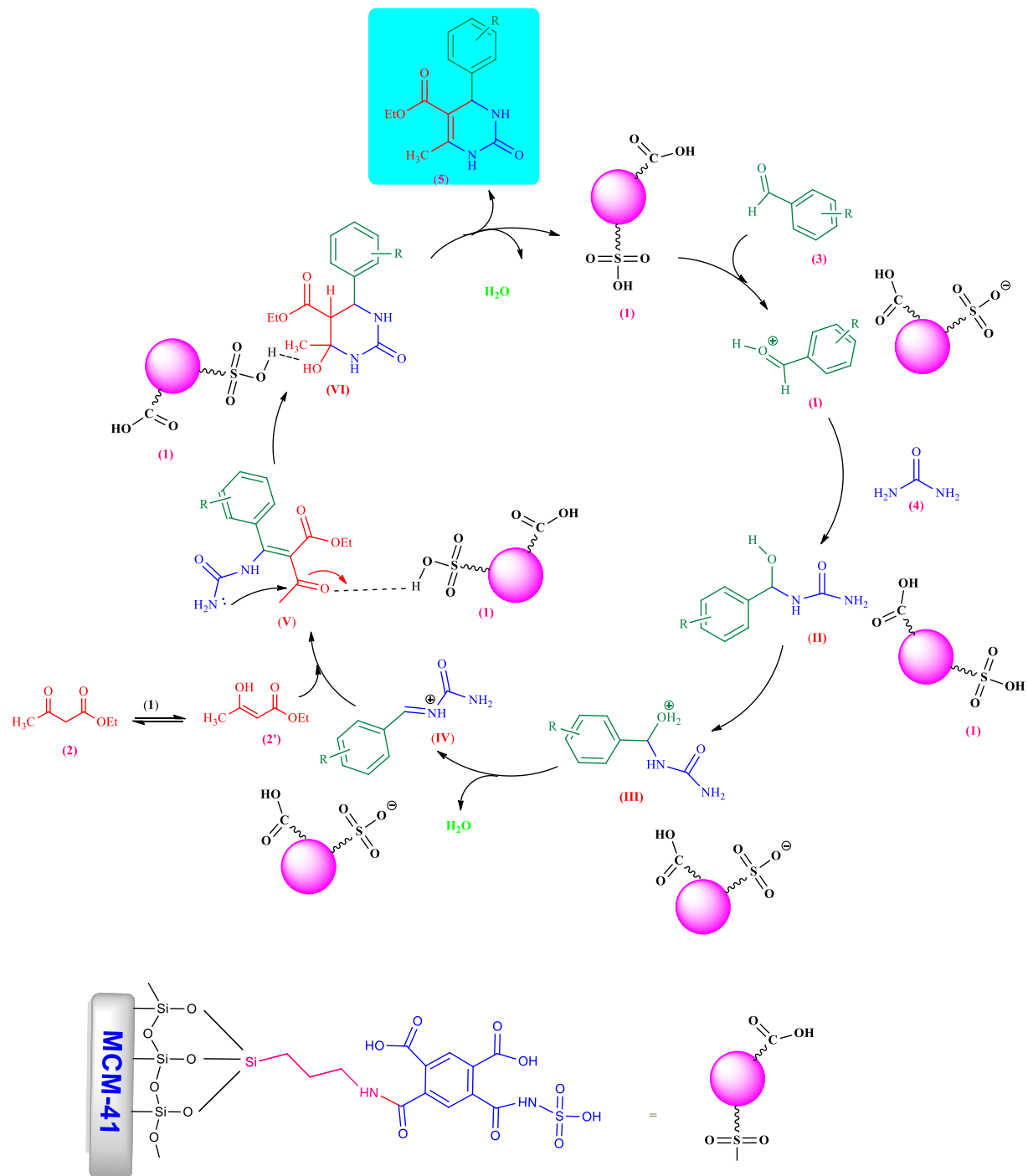
Entry	Aldehyde 3	Product 5	Time (min)	Yield (%) ^b	mp °C (Obs.)	mp °C (Lit.)
7	4-OHC ₆ H ₄ -	 (5g)	55	82	234–236	233–235 ⁷⁷
8	2-C ₄ H ₃ S-	 (5h)	45	84	212–214	210–212 ⁷⁸
9	4-Me ₂ NC ₆ H ₄ -	 (5i)	45	92	213–215	213–215 ⁷⁹
10	4-FC ₆ H ₄ -	 (5j)	60	85	180	180 ⁸⁰
11	4-OH-3-MeO-C ₆ H ₃ -	 (5k)	40	84	188–190	188.5 ⁸¹

Table 2. Scope of the Biginelli condensation for the synthesis of 3,4-dihydropyrimidin-2-(1*H*)-ones catalyzed by MCM-41-APS-PMDA-NHSO₃H (1)^a.



^aReaction conditions: ethyl acetoacetate (2, 1 mmol), aldehydes (3a–k, 1 mmol), urea (4, 1.2 mmol), MCM-41-APS-PMDA-NHSO₃H (1, 15 mg) under solvent-free conditions at 80 °C. ^bIsolated yields were reported.



Scheme 2. Proposed mechanism for the synthesis of 3,4-dihydropyrimidin-2(1H)-ones catalyzed by MCM-41 (MCM-41-APS-PMDA-NHSO₃H (1)).

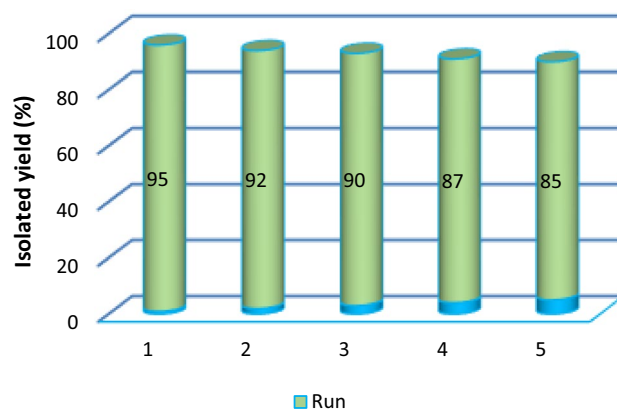


Figure 7. Reusability of the heterogeneous acidic nanocatalyst MCM-41-APS-PMDA-NHSO₃H (1) for the synthesis of 5a.

Entry	Catalyst	Amount of catalyst loading	Solvent	Temp. (°C)	Time (min)	Yield (%)	References
1	PPF-SO ₃ H	250 mg	EtOH	Reflux	480	81	⁷³
2	PANI-FeCl ₃	200 mg	CH ₃ CN	Reflux	1440	83	⁸²
3	Fe ₃ O ₄ /PAA-SO ₃ H	60 mg	Solvent-free	RT	120	90	⁸³
4	H ₂ SO ₄ -Silica gel	30 mol % (47 mg)	Solvent-free	60 °C	120	89	⁸⁴
5	Zr(H ₂ PO ₄) ₂	7 mol % (20 mg)	Solvent-free	90 °C	60	92	⁸⁵
6	MCM-41-APS-PMDA-NHSO ₃ H	15 mg	Solvent-free	80 °C	35	96	This work

Table 3. Comparison of the catalytic activity of the MCM-41-APS-PMDA-NHSO₃H (1) with other catalysts.

Received: 11 January 2021; Accepted: 28 April 2021

Published online: 27 May 2021

References

- AbuKhadra, M. R., Mohamed, A. S., El-Sherbeeney, A. M. & Elmeligy, M. A. Enhanced photocatalytic degradation of acephate pesticide over MCM-41/Co₃O₄ nanocomposite synthesized from rice husk silica gel and Peach leaves. *J. Hazard. Mater.* **389**, 122129. <https://doi.org/10.1016/j.jhazmat.2020.122129> (2020).
- Rout, L., Mohan, A., Thomas, A. M. & Ha, C.-S. Rational design of thermoresponsive functionalized MCM-41 and their decoration with bimetallic Ag-Pd nanoparticles for catalytic application. *Microporous Mesoporous Mater.* **291**, 109711. <https://doi.org/10.1016/j.micromeso.2019.109711> (2020).
- Ramazani, Z., Elhamifar, D., Norouzi, M. & Mirbagheri, R. Magnetic mesoporous MCM-41 supported boric acid: A novel, efficient and ecofriendly nanocomposite. *Compos. B Eng.* **164**, 10–17. <https://doi.org/10.1016/j.compositesb.2018.11.063> (2019).
- Björklund, S. & Kocherbitov, V. Alcohols react with MCM-41 at room temperature and chemically modify mesoporous silica. *Sci. Rep.* **7**, 9960. <https://doi.org/10.1038/s41598-017-10090-x> (2017).
- Hajjami, M., Shiri, L. & Jahanbakhshi, A. Zirconium oxide complex-functionalized MCM-41 nanostructure: An efficient and reusable mesoporous catalyst for oxidation of sulfides and oxidative coupling of thiols using hydrogen peroxide. *Appl. Organomet. Chem.* **29**, 668–673. <https://doi.org/10.1002/aoc.3348> (2015).
- Karthikyan, G. & Pandurangan, A. Heteropolyacid (H₃PW₁₂O₄₀) supported MCM-41: An efficient solid acid catalyst for the green synthesis of xanthenedione derivatives. *J. Mol. Catal. A Chem.* **311**, 36–45. <https://doi.org/10.1016/j.molcata.2009.06.020> (2009).
- Mandal, M., Nagaraju, V., Sarma, B., Karunakar, G. & Bania, K. K. Enantioselective epoxidation of styrene by manganese chiral schiff base complexes immobilized on MCM-41. *ChemPlusChem* **80**, 749–761. <https://doi.org/10.1002/cplu.201402446> (2015).
- Reddy, G. R. *et al.* Removal of organic pollutants in water by the MCM-41 anchored with nickel (II) and copper (II) complexes. *Environ. Technol. Innov.* <https://doi.org/10.1016/j.eti.2021.101492> (2021).
- Nowicki, J., Jaroszewska, K., Nowakowska-Bogdan, E., Szmatoła, M. & Howska, J. Synthesis of 2, 2, 4-trimethyl-1, 2-H-dihydroquinoline (TMQ) over selected organosulfonic acid silica catalysts: Selectivity aspects. *Mol. Catal.* **454**, 94–103. <https://doi.org/10.1016/j.mcat.2018.05.016> (2018).
- Kuboňová, L. *et al.* Catalytic activity of cobalt grafted on ordered mesoporous silica materials in N₂O decomposition and CO oxidation. *Mol. Catal.* **437**, 57–72. <https://doi.org/10.1016/j.mcat.2017.04.037> (2017).
- Sun, Z., Cui, G., Li, H., Tian, Y. & Yan, S. Multifunctional dendritic mesoporous silica nanospheres loaded with silver nanoparticles as a highly active and recyclable heterogeneous catalyst. *Colloids Surf. A* **489**, 142–153. <https://doi.org/10.1016/j.colsurfa.2015.10.052> (2016).
- Macquarrie, D. J. & Mena Durán, C. J. In *Sustainable Catalysis: Without Metals or Other Endangered Elements, Part 1* 65–78 (The Royal Society of Chemistry, 2016). <https://doi.org/10.1039/9781782622093-00065>.
- Andas, J., Ekbal, S. H. & Ali, T. H. MCM-41 modified heterogeneous catalysts from rice husk for selective oxidation of styrene into benzaldehyde. *Environ. Technol. Innov.* **21**, 101308. <https://doi.org/10.1016/j.eti.2020.101308> (2021).

14. Amolegbe, S. A. *et al.* Mesoporous silica nanocarriers encapsulated antimalarials with high therapeutic performance. *Sci. Rep.* **8**, 3078. <https://doi.org/10.1038/s41598-018-21351-8> (2018).
15. Stewart, C. A., Finer, Y. & Hatton, B. D. Drug self-assembly for synthesis of highly-loaded antimicrobial drug-silica particles. *Sci. Rep.* **8**, 895. <https://doi.org/10.1038/s41598-018-19166-8> (2018).
16. Shevtsov, M. A. *et al.* Zero-valent Fe confined mesoporous silica nanocarriers (Fe(0) @ MCM-41) for targeting experimental orthotopic glioma in rats. *Sci. Rep.* **6**, 29247. <https://doi.org/10.1038/srep29247> (2016).
17. Brezoiu, A.-M. *et al.* Heteroatom modified MCM-41-silica carriers for Lomefloxacin delivery systems. *Microporous Mesoporous Mater.* **275**, 214–222. <https://doi.org/10.1016/j.micromeso.2018.08.031> (2019).
18. Omar, H. *et al.* Impact of pore-walls ligand assembly on the biodegradation of mesoporous Organosilica nanoparticles for controlled drug delivery. *ACS Omega* **3**, 5195–5201. <https://doi.org/10.1021/acsomega.8b00418> (2018).
19. Qi, R. *et al.* Humidity sensors based on MCM-41/polypyrrole hybrid film via in-situ polymerization. *Sens. Actuators B Chem.* **277**, 584–590. <https://doi.org/10.1016/j.snb.2018.09.062> (2018).
20. Yang, Y., Hu, J. & He, J. Mesoporous nano-silica serves as the degradation inhibitor in polymer dielectrics. *Sci. Rep.* **6**, 28749. <https://doi.org/10.1038/srep28749> (2016).
21. Macquarrie, D. J. & Hu, W. In *Sol-Gel Methods for Materials Processing* (eds Innocenzi, P. *et al.*) 187–194 (Springer, 2008).
22. Lu, D. *et al.* Adsorption and desorption behaviors of antibiotic ciprofloxacin on functionalized spherical MCM-41 for water treatment. *J. Clean. Prod.* **264**, 121644. <https://doi.org/10.1016/j.jclepro.2020.121644> (2020).
23. Guo, Y., Chen, B., Zhao, Y. & Yang, T. Fabrication of the magnetic mesoporous silica Fe-MCM-41-A as efficient adsorbent: Performance, kinetics and mechanism. *Sci. Rep.* **11**, 1–12. <https://doi.org/10.1038/s41598-021-81928-8> (2021).
24. Viscardi, R., Barbarossa, V., Maggi, R. & Pancrazzi, F. Effect of acidic MCM-41 mesoporous silica functionalized with sulfonic acid groups catalyst in conversion of methanol to dimethyl ether. *Energy Rep.* **6**, 49–55. <https://doi.org/10.1016/j.egyrs.2020.10.042> (2020).
25. Martínez-Edo, G., Balmori, A., Pontón, I., Martidel Rio, A. & Sánchez-García, D. Functionalized ordered mesoporous silicas (MCM-41): Synthesis and applications in catalysis. *Catalysts* **8**, 617. <https://doi.org/10.3390/catal8120617> (2018).
26. Rizzi, V. *et al.* Amino grafted MCM-41 as highly efficient and reversible ecofriendly adsorbent material for the Direct Blue removal from wastewater. *J. Mol. Liq.* **273**, 435–446. <https://doi.org/10.1016/j.molliq.2018.10.060> (2019).
27. Wilson, K. & Lee, A. F. Catalyst design for biorefining. *Philos. Trans. R. Soc. A Math. Phys. Eng. Sci.* **374**, 20150081. <https://doi.org/10.1098/rsta.2015.0081> (2016).
28. Abu-Zied, B. M., Alam, M., Asiri, A. M., Schwieger, W. & Rahman, M. M. Fabrication of 1, 2-dichlorobenzene sensor based on mesoporous MCM-41 material. *Colloids Surf. A* **562**, 161–169. <https://doi.org/10.1016/j.colsurfa.2018.11.024> (2019).
29. Luque, R. & Clark, J. H. Valorisation of food residues: Waste to wealth using green chemical technologies. *Sustain. Chem. Process.* **1**, 10. <https://doi.org/10.1186/2043-7129-1-10> (2013).
30. Ghorbani-Choghamarani, A., Tahmasbi, B., Hudson, R. H. & Heidari, A. Supported organometallic palladium catalyst into mesoporous channels of magnetic MCM-41 nanoparticles for phosphine-free CC coupling reactions. *Microporous Mesoporous Mater.* **284**, 366–377. <https://doi.org/10.1016/j.micromeso.2019.04.061> (2019).
31. Iwanami, K., Seo, H., Choi, J.-C., Sakakura, T. & Yasuda, H. Al-MCM-41 catalyzed three-component Strecker-type synthesis of α -aminonitriles. *Tetrahedron* **66**, 1898–1901. <https://doi.org/10.1016/j.tet.2010.01.001> (2010).
32. Karami, S., Dekamin, M. G., Valiey, E. & Shakib, P. DABA MNPs: A new and efficient magnetic bifunctional nanocatalyst for the green synthesis of biologically active pyrano[2,3-c]pyrazole and benzylpyrazolyl coumarin derivatives. *New J. Chem.* **44**, 13952–13961. <https://doi.org/10.1039/D0NJ02666B> (2020).
33. Dekamin, M. G., Mokhtari, Z. & Karimi, Z. Nano-ordered B-MCM-41: An efficient and recoverable solid acid catalyst for three-component Strecker reaction of carbonyl compounds, amines and TMSCN. *Sci. Iran.* **18**, 1356–1364. <https://doi.org/10.1016/j.scient.2011.11.005> (2011).
34. Yaghoubi, A., Dekamin, M. G. & Karimi, B. Propylsulfonic acid-anchored isocyanurate-based periodic mesoporous organosilica (PMO-ICS-PrSO₃H): A highly efficient and recoverable nanoporous catalyst for the one-pot synthesis of substituted polyhydroquinolines. *Catal. Lett.* **147**, 2656–2663. <https://doi.org/10.1007/s10562-017-2159-5> (2017).
35. Yaghoubi, A., Dekamin, M. G., Arefi, E. & Karimi, B. Propylsulfonic acid-anchored isocyanurate-based periodic mesoporous organosilica (PMO-ICS-Pr-SO₃H): A new and highly efficient recoverable nanoporous catalyst for the one-pot synthesis of bis(indolyl) methane derivatives. *J. Colloid Interface Sci.* **505**, 956–963. <https://doi.org/10.1016/j.jcis.2017.06.055> (2017).
36. Akbari, A., Dekamin, M. G., Yaghoubi, A. & Naimi-Jamal, M. R. Novel magnetic propylsulfonic acid-anchored isocyanurate-based periodic mesoporous organosilica (Iron oxide@PMO-ICS-PrSO₃H) as a highly efficient and reusable nanoreactor for the sustainable synthesis of imidazopyrimidine derivatives. *Sci. Rep.* **10**, 10646. <https://doi.org/10.1038/s41598-020-67592-4> (2020).
37. Dekamin, M. G. & Mokhtari, Z. Highly efficient and convenient Strecker reaction of carbonyl compounds and amines with TMSCN catalyzed by MCM-41 anchored sulfonic acid as a recoverable catalyst. *Tetrahedron* **68**, 922–930. <https://doi.org/10.1016/j.tet.2011.10.087> (2012).
38. Choudhary, D., Paul, S., Gupta, R. & Clark, J. H. Catalytic properties of several palladium complexes covalently anchored onto silica for the aerobic oxidation of alcohols. *Green Chem.* **8**, 479–482. <https://doi.org/10.1039/B601363E> (2006).
39. Gupta, P., Kour, M., Paul, S. & Clark, J. H. Ionic liquid coated sulfonated carbon/silica composites: Novel heterogeneous catalysts for organic syntheses in water. *RSC Adv.* **4**, 7461–7470. <https://doi.org/10.1039/C3RA45229H> (2014).
40. Fathi, M., Naimi-Jamal, M. R., Dekamin, M. G., Panahi, L. & Demchuk, O. M. A straightforward, environmentally beneficial synthesis of spiro[diindeno[1,2-b:2',1'-e]pyridine-11,3'-indoline]-2',10,12-triones mediated by a nano-ordered reusable catalyst. *Sci. Rep.* **11**, 4820. <https://doi.org/10.1038/s41598-021-84209-6> (2021).
41. Avila-Ortiz, C. G. & Juaristi, E. Novel methodologies for chemical activation in organic synthesis under solvent-free reaction conditions. *Molecules* **25**, 3579. <https://doi.org/10.3390/molecules25163579> (2020).
42. Martins, M. A., Frizzo, C. P., Moreira, D. N., Buriol, L. & Machado, P. Solvent-free heterocyclic synthesis. *Chem. Rev.* **109**, 4140–4182. <https://doi.org/10.1021/cr9001098> (2009).
43. Gawande, M. B., Bonifácio, V. D. B., Luque, R., Branco, P. S. & Varma, R. S. Solvent-free and catalysts-free chemistry: A benign pathway to sustainability. *ChemSuschem* **7**, 24–44. <https://doi.org/10.1002/cssc.201300485> (2014).
44. Kaur, R., Chaudhary, S., Kumar, K., Gupta, M. K. & Rawal, R. K. Recent synthetic and medicinal perspectives of dihydropyrimidones: A review. *Eur. J. Med. Chem.* **132**, 108–134. <https://doi.org/10.1016/j.ejmech.2017.03.025> (2017).
45. Dömling, A., Wang, W. & Wang, K. Chemistry and biology of multicomponent reactions. *Chem. Rev.* **112**, 3083–3135. <https://doi.org/10.1021/cr100233r> (2012).
46. Dekamin, M. G. & Eslami, M. Highly efficient organocatalytic synthesis of diverse and densely functionalized 2-amino-3-cyano-4H-pyrans under mechanochemical ball milling. *Green Chem.* **16**, 4914–4921. <https://doi.org/10.1039/C4GC00411F> (2014).
47. Dekamin, M. G., Azimoshan, M. & Ramezani, L. Chitosan: A highly efficient renewable and recoverable bio-polymer catalyst for the expeditious synthesis of α -amino nitriles and imines under mild conditions. *Green Chem.* **15**, 811–820. <https://doi.org/10.1039/C3GC36901C> (2013).
48. Dekamin, M. G., Alikhani, M., Emami, A., Ghafuri, H. & Javanshir, S. An efficient catalyst- and solvent-free method for the synthesis of medicinally important dihydropyran[2,3-c]pyrazole derivatives using ball milling technique. *J. Iran. Chem. Soc.* **13**, 591–596. <https://doi.org/10.1007/s13738-015-0793-7> (2016).

49. Matos, L. H. S., Masson, F. T., Simeoni, L. A. & Homem-de-Mello, M. Biological activity of dihydropyrimidinone (DHPM) derivatives: A systematic review. *Eur. J. Med. Chem.* **143**, 1779–1789. <https://doi.org/10.1016/j.ejmech.2017.10.073> (2018).
50. Fard, M. A. D., Ghafuri, H. & Rashidzadeh, A. Sulfonated highly ordered mesoporous graphitic carbon nitride as a super active heterogeneous solid acid catalyst for Biginelli reaction. *Microporous Mesoporous Mater.* **274**, 83–93. <https://doi.org/10.1016/j.micromeso.2018.07.030> (2019).
51. Elhamifar, D., Hosseini, F., Karimi, B. & Hajati, S. Ionic liquid-based ordered mesoporous organosilica-supported copper as a novel and efficient nanocatalyst for the one-pot synthesis of Biginelli products. *Microporous Mesoporous Mater.* **204**, 269–275. <https://doi.org/10.1016/j.micromeso.2014.11.011> (2015).
52. de Souza, V. P. *et al.* Hybrid 3, 4-dihydropyrimidin-2-(thio) ones as dual-functional bioactive molecules: Fluorescent probes and cytotoxic agents to cancer cells. *New J. Chem.* **44**, 12440–12451. <https://doi.org/10.1039/D0NJ01368D> (2020).
53. Rao, G. D., Anjaneyulu, B. & Kaushik, M. Greener and expeditious one-pot synthesis of dihydropyrimidinone derivatives using non-commercial β -ketoesters via the Biginelli reaction. *RSC Adv.* **4**, 43321–43325. <https://doi.org/10.1039/C4RA06587E> (2014).
54. Singhal, S., Joseph, J. K., Jain, S. L. & Sain, B. Synthesis of 3, 4-dihydropyrimidinones in the presence of water under solvent free conditions using conventional heating, microwave irradiation/ultrasound. *Green Chem. Lett. Rev.* **3**, 23–26. <https://doi.org/10.1080/17518250903490126> (2010).
55. Sharma, V., Chitranshi, N. & Agarwal, A. K. Significance and biological importance of pyrimidine in the microbial world. *Int. J. Med. Chem.* <https://doi.org/10.1155/2014/202784> (2014).
56. Wan, J.-P. & Liu, Y. Synthesis of dihydropyrimidinones and thiones by multicomponent reactions: Strategies beyond the classical Biginelli reaction. *Synthesis* **2010**, 3943–3953 (2010).
57. Heravi, M. M., Asadi, S. & Lashkariani, B. M. Recent progress in asymmetric Biginelli reaction. *Mol. Divers.* **17**, 389–407. <https://doi.org/10.1055/s-0030-1258290> (2013).
58. Huang, Y., Yang, F. & Zhu, C. Highly Enantioselective Biginelli Reaction Using a New Chiral Ytterbium Catalyst: Asymmetric Synthesis of Dihydropyrimidines. *J. Am. Chem. Soc.* **127**, 16386–16387. <https://doi.org/10.1021/ja056092f> (2005).
59. Jadhav, C. K. *et al.* Efficient rapid access to Biginelli for the multicomponent synthesis of 1, 2, 3, 4-tetrahydropyrimidines in room-temperature diisopropyl ethyl ammonium acetate. *ACS Omega* **4**, 22313–22324. <https://doi.org/10.1021/acsomega.9b02286> (2019).
60. Doustkhah, E. *et al.* Development of sulfonic-acid-functionalized mesoporous materials: Synthesis and catalytic applications. *Chem. A Eur. J.* **25**, 1614–1635. <https://doi.org/chem201802183> (2019).
61. Pramanik, M. & Bhaumik, A. Phosphonic acid functionalized ordered mesoporous material: A new and ecofriendly catalyst for one-pot multicomponent Biginelli reaction under solvent-free conditions. *ACS Appl. Mater. Interfaces* **6**, 933–941. <https://doi.org/10.1021/am404298a> (2014).
62. Vekariya, R. H., Prajapati, N. P. & Patel, H. D. MCM-41-anchored sulfonic acid (MCM-41-SO₃H): An efficient heterogeneous catalyst for green organic synthesis. *Synth. Commun.* **46**, 1713–1734. <https://doi.org/10.1080/00397911.2016.1212380> (2016).
63. Dekamin, M. G., Mehdipoor, F. & Yaghoubi, A. 1,3,5-Tris(2-hydroxyethyl)isocyanurate functionalized graphene oxide: A novel and efficient nanocatalyst for the one-pot synthesis of 3,4-dihydropyrimidin-2(1H)-ones. *New J. Chem.* **41**, 6893–6901. <https://doi.org/10.1039/C7NJ00632B> (2017).
64. Alirezvani, Z., Dekamin, M. G., Davoodi, F. & Valiey, E. Melamine-functionalized chitosan: A new bio-based reusable bifunctional organocatalyst for the synthesis of cyanocinnamitrile intermediates and densely functionalized nicotinonitrile derivatives. *ChemistrySelect* **3**, 10450–10463. <https://doi.org/10.1002/slct.201802010> (2018).
65. Alirezvani, Z., Dekamin, M. G. & Valiey, E. Cu (II) and magnetite nanoparticles decorated melamine-functionalized chitosan: A synergistic multifunctional catalyst for sustainable cascade oxidation of benzyl alcohols/Knoevenagel condensation. *Sci. Rep.* **9**, 17758. <https://doi.org/10.1038/s41598-019-53765-3> (2019).
66. Alirezvani, Z., Dekamin, M. G. & Valiey, E. New hydrogen-bond-enriched 1, 3, 5-tris (2-hydroxyethyl) isocyanurate covalently functionalized MCM-41: An efficient and recoverable hybrid catalyst for convenient synthesis of acridinedione derivatives. *ACS Omega* **4**, 20618–20633. <https://doi.org/10.1021/acsomega.9b02755> (2019).
67. Banakar, S. H., Dekamin, M. G. & Yaghoubi, A. Selective and highly efficient synthesis of xanthenedione or tetraketone derivatives catalyzed by ZnO nanorod-decorated graphene oxide. *New J. Chem.* **42**, 14246–14262. <https://doi.org/10.1039/C8NJ01053F> (2018).
68. Dekamin, M. G., Arefi, E. & Yaghoubi, A. Isocyanurate-based periodic mesoporous organosilica (PMO-ICS): A highly efficient and recoverable nanocatalyst for the one-pot synthesis of substituted imidazoles and benzimidazoles. *RSC Adv.* **6**, 86982–86988. <https://doi.org/10.1039/C6RA14550G> (2016).
69. Valiey, E., Dekamin, M. G. & Alirezvani, Z. Melamine-modified chitosan materials: An efficient and recyclable bifunctional organocatalyst for green synthesis of densely functionalized bioactive dihydropyran [2, 3-c] pyrazole and benzylpyrazolyl coumarin derivatives. *Int. J. Biol. Macromol.* **129**, 407–421. <https://doi.org/10.1016/j.ijbiomac.2019.01.027> (2019).
70. Sam, M., Dekamin, M. G. & Alirezvani, Z. Dendrons containing boric acid and 1,3,5-tris(2-hydroxyethyl)isocyanurate covalently attached to silica-coated magnetite for the expeditious synthesis of Hantzsch esters. *Sci. Rep.* **11**, 4820. <https://doi.org/10.1038/s41598-020-80884-z> (2021).
71. Bharathi, M., Indira, S., Vinoth, G. & Bharathi, K. S. Immobilized Ni-Schiff-base metal complex on MCM-41 as a heterogeneous catalyst for the green synthesis of benzimidazole derivatives using glycerol as a solvent. *J. Porous Mater.* **26**, 1377–1390. <https://doi.org/10.1007/s10934-019-00736-8> (2019).
72. Romanelli, G. P., Sathicq, A. G., Autino, J. C., Baronetti, G. & Thomas, H. J. Solvent-free approach to 3, 4-dihydropyrimidin-2 (1H)-(thio) ones: Biginelli reaction catalyzed by a Wells–Dawson reusable heteropolyacid. *Synth. Commun.* **37**, 3907–3916. <https://doi.org/10.1080/00397910701572332> (2007).
73. Patel, H. A., Sawant, A. M., Rao, V. J., Patel, A. L. & Bedekar, A. V. Polyaniline supported FeCl₃: An effective heterogeneous catalyst for Biginelli reaction. *Catal. Lett.* **147**, 2306–2312. <https://doi.org/10.1007/s10562-017-2139-9> (2017).
74. Safaei-Ghomi, J., Tavazo, M. & Mahdavinia, G. H. Ultrasound promoted one-pot synthesis of 3, 4-dihydropyrimidin-2 (1H)-ones/thiones using dendrimer-attached phosphotungstic acid nanoparticles immobilized on nanosilica. *Ultrason. Sonochem.* **40**, 230–237. <https://doi.org/10.1016/j.ultsonch.2017.07.015> (2018).
75. Hosseini, M. M., Kolvari, E., Koukabi, N., Ziyaei, M. & Zolfogol, M. A. Zirconia sulfuric acid: An efficient heterogeneous catalyst for the one-pot synthesis of 3, 4-dihydropyrimidinones under solvent-free conditions. *Catal. Lett.* **146**, 1040–1049. <https://doi.org/10.1007/s10562-016-1723-8> (2016).
76. Li, W., Zhou, G. & Zhang, P. One-pot synthesis of dihydropyrimidinones via environmentally friendly enzyme-catalyzed Biginelli reaction. *Heterocycles* **83**, 2067–2077. <https://doi.org/10.3987/COM-11-12267> (2011).
77. Ghafuri, H. & Talebi, M. Water-soluble phosphated graphene: Preparation, characterization, catalytic reactivity, and adsorption property. *Ind. Eng. Chem. Res.* **55**, 2970–2982. <https://doi.org/10.1021/acs.iecr.5b02250> (2016).
78. Wang, D.-C., Guo, H.-M. & Qu, G.-R. Efficient, green, solvent-free synthesis of 3, 4-dihydropyrimidin-2 (1H)-ones via Biginelli reaction catalyzed by Cu(NO₃)₂·3H₂O. *Synth. Commun.* **40**, 1115–1122. <https://doi.org/10.1080/00397910903043009> (2010).
79. Kolvari, E., Koukabi, N., Hosseini, M. M., Vahidian, M. & Ghobadi, E. Nano-ZrO₂ sulfuric acid: A heterogeneous solid acid nano catalyst for Biginelli reaction under solvent free conditions. *RSC Adv.* **6**, 7419–7425. <https://doi.org/10.1039/C5RA19350H> (2016).
80. Khiratkar, A. G., Muskawar, P. N. & Bhagat, P. R. Polymer-supported benzimidazolium based ionic liquid: An efficient and reusable Brønsted acid catalyst for Biginelli reaction. *RSC Adv.* **6**, 105087–105093. <https://doi.org/10.1039/C6RA23781A> (2016).

81. Mahato, B. N. & Krithiga, T. Mesoporous ZnO/AlSBA-15 (7) nanocomposite as an efficient catalyst for synthesis of 3, 4-dihydropyrimidin-2 (1H)-one via Biginelli reaction and their biological activity study. *Bull. Chem. React. Eng. Catal.* **14**, 634–645. <https://doi.org/10.9767/bcrec.14.3.4469.634-645> (2019).
82. Zamani, F. & Izadi, E. Synthesis and characterization of sulfonated-phenylacetic acid coated Fe₃O₄ nanoparticles as a novel acid magnetic catalyst for Biginelli reaction. *Catal. Commun.* **42**, 104–108. <https://doi.org/10.1016/j.catcom.2013.08.006> (2013).
83. Salehi, P., Dabiri, M., Zolfigol, M. A. & Bodaghi Fard, M. A. Efficient synthesis of 3, 4-dihydropyrimidin-2 (1H)-ones over silica sulfuric acid as a reusable catalyst under solvent-free conditions. *Heterocycles* **60**, 2435–2440. <https://doi.org/10.3987/COM-03-9837> (2003).
84. Tamaddon, F. & Moradi, S. Controllable selectivity in Biginelli and Hantzsch reactions using nanoZnO as a structure base catalyst. *J. Mol. Catal. A Chem.* **370**, 117–122. <https://doi.org/10.1016/j.molcata.2012.12.005> (2013).
85. Küçükislaınođlu, M., Beşoluk, Ş, Zengin, M., Arslan, M. & Nebiođlu, M. An efficient one-pot synthesis of dihydropyrimidinones catalyzed by zirconium hydrogen phosphate under solvent-free conditions. *Turk. J. Chem.* **34**, 411–416. <https://doi.org/10.3906/kim-0912-357> (2010).
86. Dekamin, M. G., Karimi, Z. & Farahmand, M. Tetraethylammonium 2-(N-hydroxycarbamoyl) benzoate: A powerful bifunctional metal-free catalyst for efficient and rapid cyanosilylation of carbonyl compounds under mild conditions. *Catal. Sci. Technol.* **2**, 1375–1381. <https://doi.org/10.1039/C2CY20037F> (2012).

Acknowledgements

We are grateful for the financial support from The Research Council of Iran University of Science and Technology (IUST), Tehran, Iran (Grant No 160/19108). We would also like to acknowledge the support of the Iran Nanotechnology Initiative Council (INIC).

Author contributions

E.V. worked on the topic as his Ph.D Thesis and prepared the initial draft of the manuscript. Prof. M.G.D. is the supervisor of Mr. E.V. and Dr. Z.A., as his Ph.D students. Also, he edited and revised the manuscript completely. Dr. Z.A. worked closely with Mr. E.V. for doing experimental section and interpreting of the characterization data.

Competing interests

The authors declare no competing interests.

Additional information

Correspondence and requests for materials should be addressed to M.G.D.

Reprints and permissions information is available at www.nature.com/reprints.

Publisher's note Springer Nature remains neutral with regard to jurisdictional claims in published maps and institutional affiliations.



Open Access This article is licensed under a Creative Commons Attribution 4.0 International License, which permits use, sharing, adaptation, distribution and reproduction in any medium or format, as long as you give appropriate credit to the original author(s) and the source, provide a link to the Creative Commons licence, and indicate if changes were made. The images or other third party material in this article are included in the article's Creative Commons licence, unless indicated otherwise in a credit line to the material. If material is not included in the article's Creative Commons licence and your intended use is not permitted by statutory regulation or exceeds the permitted use, you will need to obtain permission directly from the copyright holder. To view a copy of this licence, visit <http://creativecommons.org/licenses/by/4.0/>.

© The Author(s) 2021